QUALITY ENHANCEMENT OF PROCAM SYSTEM BY RADIOMETRIC COMPENSATION

Tai-Hsiang Huang[1], Chen-Tai Kao[2], and Homer. H. Chen[1]
[1]*Graduate Institute of Communication Engineering* [2]*Department of Electrical Engineering*
National Taiwan University
Taipei, Taiwan
[d97942020, b97901112]@ntu.edu.tw Homer@cc.ee.ntu.edu.tw

ABSTRACT

A procam system consists of a projector and a camera. In this paper, a radiometric compensation scheme is proposed for improving the projection quality of a procam system that uses a nearby non-white wall as the projection screen. The compensation scheme is capable of correcting the radiometric errors such as chroma and brightness distortions caused by the projection surface and the ambient light. It is also capable of compensating the effects of nonlinear spectral response (including vignetting) of the procam system. These important functions are achieved through a computational framework that optimizes the tradeoff between chroma and brightness distortions of the projected image and accelerates the computation of the penalty in the optimization process. Experimental results are shown to demonstrate the performance of the proposed radiometric compensation scheme.

Index Terms— Procam system, vignetting, radiometric compensation.

I. INTRODUCTION

The projector technology has advanced significantly over the past years, making possible high resolution, high dynamic range display of images. In practice, it may happen that a professional projection screen is not available, so an ad hoc viewing surface, for example, a wall nearby the projector, is used as a replacement. This is particularly the case for pico projectors, which are designed to project digital images onto any nearby viewing surface. For most applications, it is important to project a clear image, regardless of the physical characteristics of the viewing surface. To achieve this goal, a camera can be incorporated into the projector to form a closed-loop system (known as procam) for enhancing the image quality.

It often happens that the ad hoc viewing wall is not pure white. A non-white surface absorbs complementary color and introduces chroma distortion to the projected image, resulting in color degradation. Conventional techniques [1]–[3] counteract this effect by increasing the intensity of the complementary color. However, because the compensated color outside the dynamic range of the projector is clipped, these techniques suffer from color distortion. To solve this problem, methods using multi-projectors to increase the dynamic range have been proposed [4]. Clearly, this solution has a higher cost because of the use of multiple projectors. The PRISM method [5] exploits the properties of human visual system to make the chroma distortion imperceptible; however, it is content-unaware and does not fully utilize the dynamic range of the projector. Methods that reduce the chroma distortion by scaling down the image intensity have been developed [4]–[7]. However, the scaling results in brightness loss and degrades the projection quality.

To preserve both chroma and brightness, we propose to simultaneously scale and boost image intensity. The scaling makes most colors in the image reproducible, while the boosting helps preserve the brightness of the image. This technique needs to balance between chroma distortion and brightness loss, for which we develop an optimization framework and a scheme to speed up the optimization process.

This paper focuses on radiometric distortions caused by a homogeneous planer surface. The resulting technique can be applied to a non-homogeneous projection surface by decomposing the surface into a number of homogeneous surfaces.

The remainder of the paper is organized as follows. Section II presents the procam system and its mathematical model. Section III presents the proposed radiometric compensation scheme. The experimental results are given in section IV. Finally, the concluding remarks are drawn in section V.

II. MODELING OF THE PROCAM SYSTEM

As shown in Fig. 1, the procam system under consideration consists of a projector, a camera, and a computer. The camera acts like an eye to sense the photometric characteristics of the projection screen and the ambient light. The resulting photometric parameters are then used to modify the input image so that the projected image looks as if it were generated by the projector on a pure white screen.

To transform a non-white surface nearby the projector into a projection screen with decent display quality, the system should be able to handle the chroma and brightness

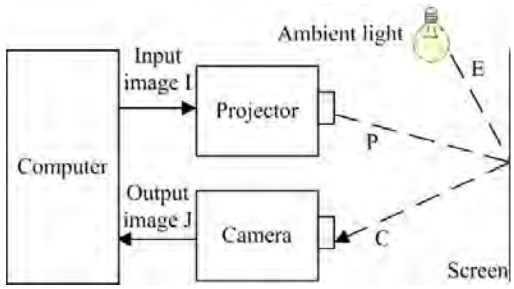

Fig. 1. The architecture of a procam system.

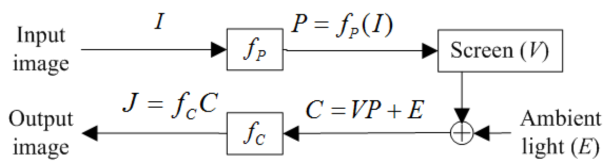

Fig. 2. Mathematical model of a procam system.

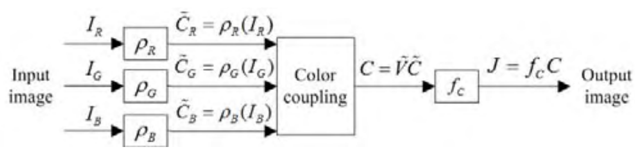

Fig. 3. The modified procam model.

distortions caused by the non-white viewing surface and the ambient light. The system should also be able to handle the nonlinear spectral responses of the projector and the camera.

To design a method that meets the above requirements, a mathematical model of the procam needs to be established that captures the characteristics of the projector transfer function, the reflectance of the screen, the influence of the ambient light, and the camera transfer function. In this work, we adopt Nayar's procam model [2] shown in Fig. 2. Suppose I is the input image and P is the projected image. Then, the model characterizes the relation between P and I by the projector's transfer function f_P,

$$P = f_P(I)\,, \tag{1}$$

where P and I are both 3-vectors. The viewing surface functions as a color modulator that converts an input color to another color. Mathematically, the color modulation operation can be represented as a 3-by-3 matrix. Since the ambient light also affects the color appearance of an image and such effect is additive, the combined color C input to the camera is described by

$$C = VP + E\,, \tag{2}$$

where E is the ambient light, and V is a 3-by-3 color modulation matrix. Finally, the output image J of the camera is related to the input image C by the camera transfer function f_C,

$$J = f_C(C)\,. \tag{3}$$

In this work we assume f_C is known. Thus, the unknowns to be determined are V, E, and the projector transfer function f_P, which is typically a nonlinear function. Determining f_P is equivalent to finding the projected image value for each possible input image value. Suppose each color component is represented by 8 bits. Since each color has 3 components, a set of 256x256x256 unknowns need to be determined. As this is a large number, determining f_P is extremely time-consuming. Grossberg *et al.* proposed a color decoupling method [2] to reduce the number of unknowns to 768. This method processes the three color channels separately by decomposing V into the multiplication of two terms as follows:

$$V = \begin{bmatrix} V_{RR} & V_{RG} & V_{RB} \\ V_{GR} & V_{GG} & V_{GB} \\ V_{BR} & V_{BG} & V_{BB} \end{bmatrix} = \begin{bmatrix} 1 & \tilde{V}_{RG} & \tilde{V}_{RB} \\ \tilde{V}_{GR} & 1 & \tilde{V}_{GB} \\ \tilde{V}_{BR} & \tilde{V}_{BG} & 1 \end{bmatrix} \begin{bmatrix} V_{RR} & 0 & 0 \\ 0 & V_{GG} & 0 \\ 0 & 0 & V_{BB} \end{bmatrix}, \tag{4}$$

Denote the first term by $\tilde{V}$ and the second term by D. Then, multiplying (2) by $\tilde{V}^{-1}$ yields

$$\tilde{C} = \tilde{V}^{-1} C\,. \tag{5}$$

Substituting (2) into (5), we have

$$\tilde{C} = \tilde{V}^{-1} VP + \tilde{V}^{-1} E = DP + \tilde{E}\,. \tag{6}$$

We can immediately see that, because D is a diagonal matrix, each color channel in P only affects the same color channel in $\tilde{C}$. Accordingly, we may simplify our mathematical model to the one shown in Fig. 3, where ρ_R, ρ_G, and ρ_B, respectively, denote the mapping functions from the 8-bit R, G, and B color intensities to the corresponding decoupled camera irradiance values. The decoupled irradiance values are then coupled and mapped by f_C to generate the output image. The coupling is the reverse process of (5).

III. METHOD

The flow chart of the proposed method is shown in Fig. 4. The whole process consists of three steps: first the camera irradiance on a white screen of the original image is estimated using the modified procam model shown in Fig. 3. Then, the estimated irradiance image is scaled down and boosted to suit the dynamic range. Finally, the modified procam model is adopted in a reversed manner to compute the compensated image, only that this time the parameters of colored instead of white screen are used. Since the first and last steps are both achieved based on the modified procam model, they will be described together in the following subsection. The limitations of the procam system and how the optimization problem is formulated based on those limitations are described in another two subsections.

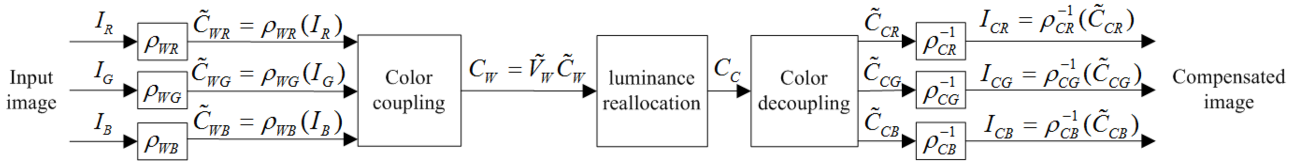

Fig. 4. Flow chart of the proposed method.

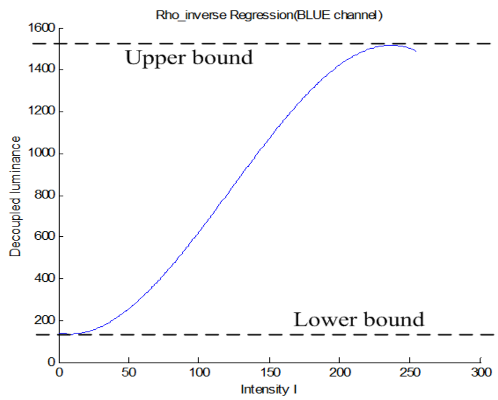

Fig. 5. The limitation of the color compensation capability of a procam system can be shown graphically on a plot of a ρ function. The blue curve in this example is the plot of the ρ function of the blue color channel of a procam system measured using a yellow screen. The range of this function is bounded between 110 and 1520. The existence of these bounds indicates that a decoupled luminance can be reproduced by this procam system only when it locates inside the bounded range.

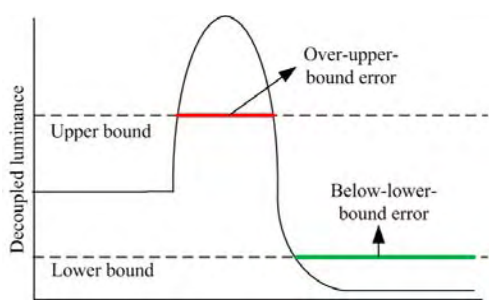

Fig. 6. Two types of errors occur when the target signal is beyond the limitation of the procam system. The top and bottom dash lines are the same bounds depicted in Fig. 5. For a target signal marked with black, the red and green line segment, respectively, represent the regions where over-upper-bound error and below-lower-bound error occur.

A. Radiometric Compensation

The modified procam model is used to estimate the irradiance image C_W on a white screen and to generate the compensated image which is to be projected on a colored screen. In the irradiance image estimation process, the model is adopted to acquire the camera irradiance, while in the compensated image generation process the model is exploited in a reverse manner to transform irradiance back to intensity. To make the notations used in Fig. 4 more distinguishable, notations corresponding to the estimation

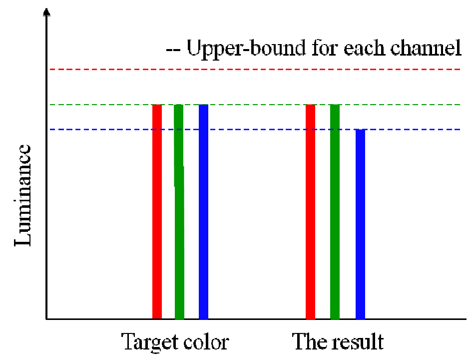

Fig. 7. Clipping phenomenon on a yellow screen. Light absorption of the screen limits the performance of the blue channel, leading to the distortion of the resulted color. In this case, target color (gray) is distorted, resulting in a yellowish color.

and the generation processes, respectively, are denoted with subscript W and C, such as C_W and C_C.

Two calibrations are performed off-line to determine the parameters needed for the whole radiometric compensation process. The first calibration is performed to determine the color coupling matrix $\tilde{V}_W$ and the mapping functions ρ_{WR},ρ_{WG}, and ρ_{WB} of the white screen, and the second calibration is performed to determine the color coupling matrix $\tilde{V}_C$ and the mapping functions ρ_{CR}, ρ_{CG}, and ρ_{CB} of the colored screen. In each calibration, the color coupling matrix is first determined using the technique described in [2]. Then, with the color coupling matrix, we apply it on an image with specially designed pixel value patterns ranging from 0 to 255 to compute the decoupled camera irradiance image. The mapping functions are then determined by pairing the decoupled camera irradiance values with their corresponding intensity values.

A. Limitations of a Procam System

Up to this point, we have determined the parameters that characterize the procam system, which means theoretically, the distortions caused by the screen and the ambient light should be fully compensated. However, limitations exist in that not all colors are reproducible on a colored screen. For example, bright luminance intensities cannot be reproduced on a totally black screen due to its low reflectance. We plot a mapping function here to better illustrate the property. In Fig. 5, the blue curve represents the mapping function of the blue color channel measured on a yellow screen. The range of this function is bounded between 110 and 1520, which are the upper and lower bounds of the decoupled luminance that can be reproduced by the procam system.

In the radiometric compensation process, the decoupled luminance values $\tilde{C}_{CR}$, $\tilde{C}_{CG}$, and $\tilde{C}_{CB}$ are clipped if their values are above the upper bound or below the lower bound (See Fig. 6.), which results in color distortion. Fig. 7 illustrates this phenomenon with R, G, and B color channels represented by red, green, and blue colors. The color bars represent the expected luminance values, while the dash lines denote the reproducible upper bounds of each channel. It can be seen that the blue channel is clipped, which yields a yellowish (the complementary color of blue) result rather than the intended gray color. In our work, the compensation errors caused by the two types of clippings are referred to as the over-upper-bound and below-lower-bound errors respectively.

C. Luminance Reallocation

To reduce the over-upper-bound error, most existing methods [4-7] scale down the dynamic range of the image to make it fall below the upper-bound. Without considering the existence of the lower-bound, these techniques inevitably introduce below-lower-bound errors. To tackle this problem, we propose to reallocate the distribution of the luminance values to make them fall within the reproducible range. The reallocation process can be described by the following linear equation:

$$C_c(x, y) = \alpha C_w(x, y) + \beta \,, \tag{7}$$

where C_w and C_c, respectively, represent the original and the new decoupled luminance values, x and y are the spatial index, α is the scaling factor, and β is the boosting factor. It should be noted that we use the same α and β for all three color channels to avoid hue distortion in the compensated image. In particular, if α and β are separately determined for different channels, each color channel will go through different reallocation process and thus results in hue distortion in the compensated image.

Intuitively, α and β should be determined such that the decoupled luminance values of all pixels fall in the reproducible decoupled luminance range to avoid the over-upper-bound and below-lower-bound errors. This strategy, unfortunately, may introduce substantial brightness loss of the compensated image because the reallocated dynamic range of all color channels are confined by the one that is most suppressed. The problem becomes more severe when the screen has highly saturated color, for example, the magenta screen shown in Fig. 1, that the reproducible luminance range of one channel is much smaller than those of the other color channels. In this case, though a small scaling factor can ensure the reproducibility all colors in the compensated image, it inevitably reduces the overall brightness. Considering the tradeoff between the color reproducibility and the brightness, we determine α and β through the following optimization process:

$$(\alpha, \beta) = \underset{\alpha,\beta}{\arg\min}\ (E_u + E_l) + \lambda E_b \,, \tag{8}$$

where E_u and E_l, respectively, accounts for the over-upper-bound and the below-lower-bound error, E_b is the penalty term accounting for brightness loss, and λ is a weighting factor. In particular, we define E_u and E_l, respectively, as the total number of pixels with decoupled luminance value larger than the upper bound and smaller than the lower bound, and E_b as the square of (1-α).

D. Acceleration Method

Originally, to obtain E_u and E_l, we need to first compute the modified decoupled luminance image C_c for each possible α and β pair and then count the number of pixels that exceed the upper bound L_u or the lower bound L_l. The procedure described above is time-consuming and not practical for real-time application. To solve this problem, we propose an acceleration method to efficiently obtain E_u and E_l.

The acceleration method is developed based on the fact that both scaling and boosting operations do not change the order of the pixel luminance values. This property allows us to skip the computation of C_c and directly obtain E_u and E_l from C_w. Specifically, given a pair of scaling and boosting factors (α_s, β_s), the number of pixels that suffer over-upper-bound error in C_c is equal to the number of pixels with luminance larger than $(L_u-\beta_s)/\alpha_s$ in C_w. Likewise, the number of pixels that suffer below-lower-bound error in C_c is equal to the number of pixels with luminance smaller than $(L_l-\beta_s)/\alpha_s$ in C_w. As a result, we can pre-compute the cumulative histogram h_c of C_w, and instead of repeating the counting process for each possible α and β pairs, the E_u and E_l can then be computed with the process described below:

$$\left(E_u, E_l\right) = \left(h_c\left(\left\lfloor \frac{L_l - \beta}{\alpha} \right\rfloor\right), N - h_c\left(\left\lceil \frac{L_u - \beta}{\alpha} \right\rceil\right)\right), \tag{9}$$

where N is the total number of pixels in C_w.

IV. EXPERIMENTAL RESULTS

We test the optimization framework using a procam system with simplified settings. In particular, the screen is diffusive and the texture on it is homogeneous. It should be noted that though the settings are simple, the system is sufficient to verify the idea behind the proposed framework. As shown in Fig. 1, our system consists of a projector (SANYO PLC-XW56) and a camera (Canon 40D). The left half side of the screen is white and the right half side is colored. The colored part of the projection surface is changeable so that we can test our radiometric compensation

Fig. 8. Experimental setup. The procam system consists of a projector (SANYO PLC-XW56) and a camera (Canon 40D).

(a) (b)

Fig. 9. Two of the test images projected on the white screen. (a) Waterfall. (b) Motorbikes.

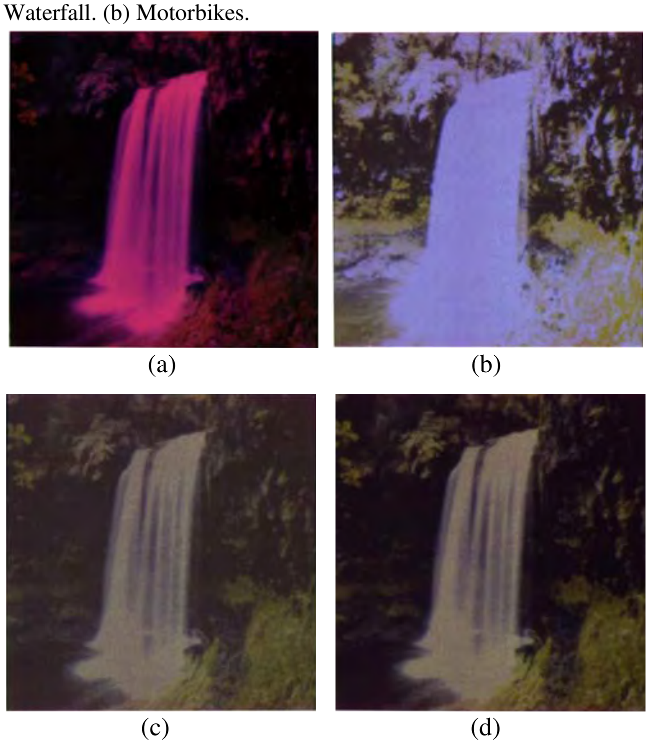

Fig. 10. 'Waterfall' projected on the magenta screen. (a) Without compensation. (b) C method. (c) CM method. (d) CMB method.

algorithm with different colors of screens. In Fig. 8, for example, the color of the screen is magenta.

Fig. 9 shows the test images, Waterfall and Motorbikes, when projected on a white screen. The Waterfall image

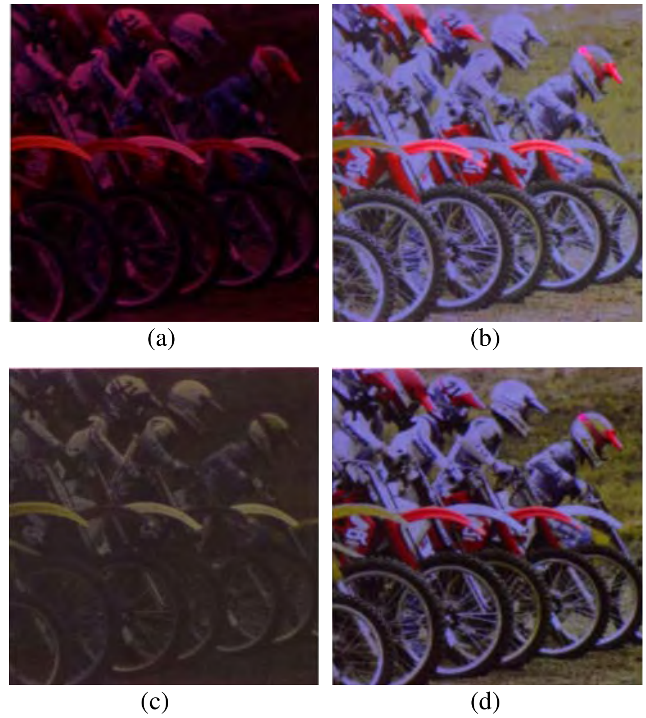

Fig. 11. Motorbikes projected on the magenta screen. (a) Without compensation. (b) C method. (c) CM method. (d) CMB method.

includes both very bright and dark regions, and the Motorbikes image features high color diversity and uniform luminance distribution. These two images serve as the reference results in this performance comparison.

We compare the results of four different types of methods: 1) Direct projection, 2) Projection with color compensation but without luminance reallocation, 3) Projection with color compensation and scaling-based luminance reallocation, and 4) Projection with color compensation using the proposed method. These methods are denoted as O, C, CM, and CMB, respectively. It should be noted that the techniques described in [1]-[3] are C type methods, and those described in [4]-[7] are CM type methods.

Figs. 10–13 show the results of the two test images on magenta and yellow screens. Without compensation, the color of Fig. 10(a) is heavily distorted due to the colored screen. Furthermore, the green background of Fig. 10(a) is darkened because, compared with red and blue, green is mostly absorbed by the magenta screen.

The results of C type methods suffer from luminance clipping of the system described in Sec. III.B. The clipping results in two kinds of artifacts: details missing and color distortion. The former artifact can be observed in the central region of Fig. 10(b), where the details of the waterfall are lost compared with those in Fig. 9(a). The latter artifact can be observed in Fig. 11(b), where the white helmet and sleeves are slightly yellowish compared with those in Fig. 9(b).

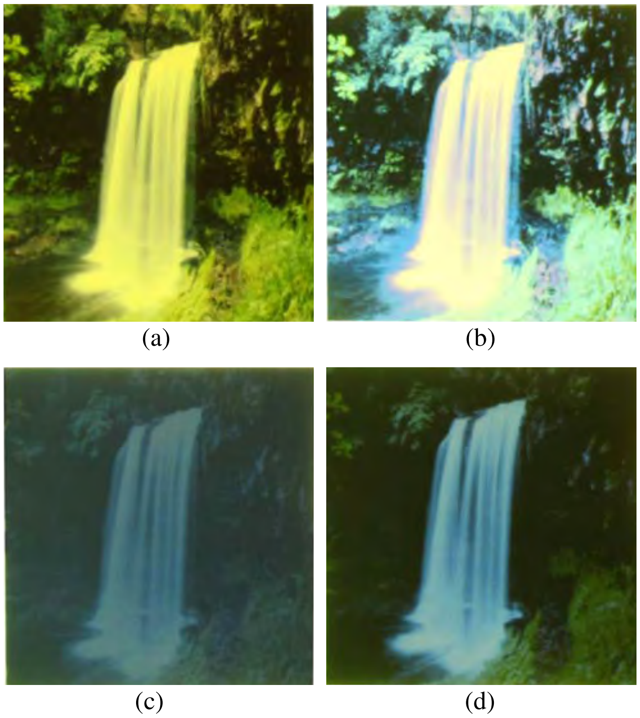

(a) (b) (c) (d)

Fig. 12. Waterfall projected on the yellow screen. (a) Without compensation. (b) C method. (c) CM method. (d) CMB method.

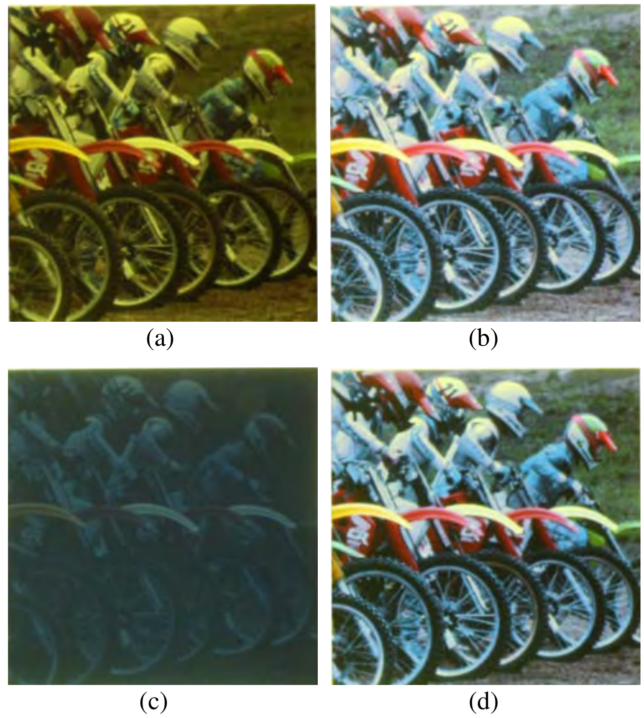

(a) (b) (c) (d)

Fig. 13. Motorbikes projected on a yellow screen. (a) Without compensation. (b) C method. (c) CM method. (d) CMB method.

The results of CM type methods suffer from brightness loss (See Figs. 10(c), 11(c), 12(c), and 13(c)). Though these figures exhibit more correct chroma, poor brightness is an obvious drawback. It should be noted that although the CM type methods work fine on screens that have low saturated colors [4]-[7], they show no more promising works when it comes to high saturated color screens.

Figs. 10(d), 11(d), 12(d), and 13(d) show the results of the proposed method. The original chroma was recovered by scaling down the image intensity, while the brightness was retained by allowing minor color distortion. It can be seen that with the optimization framework, our proposed method greatly enhances the quality of the compensated image.

V. CONCLUSION

The dynamic range of the projector is the main limiter of the radiometric compensation system. To cope with this constraint while enhancing the projection quality, we propose an optimization framework to scale and boost the image. It balances between chroma distortion and brightness loss. Experimental results show that our method preserves reasonable brightness with little chroma distortion.

Furthermore, a computational method is developed to reduce the computation of the penalty function in the optimization process. By leveraging the luminance order preserving property of the scaling and boosting operations, we only need to compute the cumulative histogram of the decoupled luminance once.

REFERENCES

[1] D. –C. Kim, T. –H. Lee, M. –H. Choi, and Y. –H. Ha, “Color correction for projected image on colored screen based on a camera,” In *Proc. SPIE-IS&T Electronic Imaging,* 2011.

[2] M. D. Grossberg, H. Peri, S. K. Nayar, and P. N. Belhumeur, “Making one object look like another: controlling appearance using a projector-camera system,” In *Proc. CVPR*, 2004.

[3] O. Bimber, A. Emmerling, and T. Klemmer, “Embedded Entertainment with Smart Projectors,” *IEEE Computer*, vol.38, pp. 48-55, 2005.

[4] A. Majumder, D. Jones, M. McCrory, M. E. Papka, and R. Stevens, “Using a camera to capture and correct spatial photometric variation in multi-projector displays,” *IEEE International Workshop on Projector-Camera Systems*, 2003.

[5] A. Majumder and M. S. Brown, “Building Large Area Displays, ” *Eurographics*, 2003.

[6] W. Zou and H. Xu, “Colorimetric color reproduction framework for screen relaxation of projection display,” Displays, vol. 32, pp. 313-319, 2011.

[7] B. Zhu, L. Xie, T. Yang, Q. Wang, and Y. Zheng, “A novel radiometric projector compensation algorithm based on lambertian reflection model,” In *Proc. SPIE,* vol.8004, 2011.